Effects of the Dirac sea on pion propagation in asymmetric nuclear matter

Subhrajyoti Biswas and Abhee K. Dutt-Mazumder
Saha Institute of Nuclear Physics, 1/AF Bidhannagar, Kolkata-700 064, India
(Received 13 April 2007; revised manuscript received 26 December 2007; published 4 April 2008)

We study pion propagation in asymmetric nuclear matter (ANM). One of the interesting consequences of pion propagation in ANM is the mode splitting for the different charged states of pions. First we describe the pion-nucleon dynamics using the nonchiral model in which one starts with pseudoscalar πN coupling, and the pseudovector representation is obtained via suitable nonlinear field transformations. For both of these cases, the effect of the Dirac sea is estimated. Subsequently, we present results using the chiral effective Lagrangian where the short-distance behavior (Dirac vacuum) is included by redefining the field parameters as done in the modern effective field theory approach developed recently. The results are compared with previous calculations for symmetric nuclear matter. Closed form analytical results are presented for the effective pion masses and dispersion relations by making a hard nucleon loop approximation and suitable density expansion.

DOI: 10.1103/PhysRevC.77.045201 PACS number(s): 21.65.Cd, 13.75.Cs, 13.75.Gx, 21.30.Fe

I. INTRODUCTION

Pions in nuclear physics assume a special status. They are responsible for the spin-isospin dependent long-range part of the nuclear force. In addition, there are variety of physical phenomena related to pion propagation in nuclear matter. One of the fascinating ideas in relation to the pion-nucleon dynamics in nuclear matter is pion condensation [1]. This might happen if there exists spacelike zero energy excitation of pionic modes. The short-range correlation, on the other hand, removes such a possibility at least at densities near the saturation densities. In the context of relativistic heavy ion collisions (RHIC), Mishustin *et al.* discussed the importance of the medium-modified pion spectrum and showed that because of the lowering of energy, the pion, in nuclear matter, might carry a bulk amount of entropy [2]. Subsequently, Gyulassy and Greiner studied pionic instability in great detail in the context of RHIC [3]. The production of pionic modes in nuclear collisions was also discussed in Ref. [4].

In experiments, the medium-dependent pion dispersion relation can also be probed via the measurements of the dilepton invariant mass spectrum. The lepton pairs produced with invariant mass near the ρ pole are sensitive to the slope of the pion dispersion relation in matter [5]. Particularly the softening of momentum dependence of the pion dispersion relation in matter leads to a higher yield of dileptons. Gale and Kapusta were first to realize that the in-medium pion dynamics can be studied by measuring lepton pair productions [6]. Most of the earlier studies of in-medium pion properties were performed in the nonrelativistic framework [7–9]. A quasirelativistic approach was taken in Refs. [10–12], in which the calculations were extended to finite temperature. In particular, Ref. [12] discusses various noncollective modes with the possibility of pion condensation. In Ref. [5], on the other hand, the dilepton production rates were calculated using nonrelativistic pion dispersion relations. Reference [13] treated the problem relativistically but used the free Fermi gas model; while in Ref. [14], pion propagation was studied by extending the Walecka model [15] and including the Δ baryon. In recent years, significant progress has been made in calculating dilepton production rates involving pionic properties in a more realistic framework [5,6,12,16–18].

In the present paper we study pion dispersion relations in asymmetric nuclear matter (ANM) using relativistic models. This is important because most of the calculations, as mentioned above, are either restricted to symmetric nuclear matter (SNM) or performed in the nonrelativistic framework. Here we focus on the propagating modes of various charged states of pions which are nondegenerate in ANM. The importance of relativistic corrections and density-dependent pion mass splitting in ANM in the context of deriving pion-nucleus optical potential was discussed in Ref. [19]. The formalism adopted in Ref. [19] was that of chiral perturbation theory. Recently, in the context of astrophysics, pionic properties in ANM have also been studied by involving the Nambu-Jona-Lasinio model [20,21]. Motivated by Ref. [19], the present authors revisited the problem in Ref. [22], where not only the static self-energy responsible for the mass splitting but also the full dispersion relations for the various charged states of pions were calculated after performing relevant density expansion in terms of the Fermi momentum. However, in our previous work [22], pions were included via straight-forward pseudovector (PV) coupling in the Walecka model [15], which renders the theory nonrenormalizable. Although the problem of nonrenormalizability could be avoided by considering the pseudoscalar (PS) πN coupling. This, on the other hand, fails to account for the pion-nucleon phenomenology.

Historically, the extension of the Walecka model to include the isovector π and ρ meson for the realistic description of dense nuclear matter (DNM) while retaining the renormalizibility of the theory was first made by Serot [23]. However, in that work, the calculation was restricted only to the mean field level, which gives rise to the tachyonic mode for pions even at density as low as $0.1\rho_0$, where ρ_0 denotes normal nuclear matter (NNM) density [24]. Such a nonpropagating mode for the pions can be removed by extending the calculation beyond the mean field level as showed by Kapusta [24]. This, in effect, means inclusion of the π-NN loop while calculating

the in-medium dressed propagator for the pion. This model has an added advantage because of the presence of π-σ coupling in addition to the usual PS coupling of the pion with the nucleons, which is responsible for the generation of small s-wave pion nucleon interaction in vacuum. This is consistent with the observed characteristics of the pion-nucleon interaction, which is dominated by p-wave scattering while the s-wave scattering length is almost zero. In matter, however, as argued in Refs. [24,25], such subtle cancellation does not occur resulting in an unrealistically large mass for the pions in matter. To circumvent this problem, it was suggested in Ref. [24] to use the pseudovector coupling even though it makes the theory nonrenormalizable.

The theoretical challenge, therefore, is to construct a model with the πN PV interaction, which preserves the renormalizability of the theory. This was accomplished in Ref. [25] following the technique developed by Weinberg [26–28] and Schwinger [29]. Here one starts with the PS coupling and subsequently invokes nonlinear field transformations to obtain PV representation. Unlike the straight-forward inclusion of the PV interaction, in this method one requires only a finite number of counterterms, which makes the theory renormalizable. Here we start with this model developed by Matsui and Serot [25] to study pion propagation in ANM. Clearly, the model adopted here is different from what we had invoked in our previous work [22]. Furthermore, in Ref. [22], for the determination of pion self-energy in matter, only the scattering from the Fermi sphere was considered and the vacuum part was completely ignored. The latter gives rise to a large contribution to the pion self-energy in presence of strong scalar density (ρ_s).

The above-mentioned model has various shortcomings too. In fact, Ref. [25] itself discusses its limitations in describing many-body πN dynamics. For example, the successful description of the saturation properties of nuclear matter in this scheme requires higher scalar mass, which gives rise to larger in-medium nucleon mass compared to the mean field theory. In addition, it also fails to account for the observed pion-nucleus scattering length at finite density [25]. In the same work, the chiral π-σ model is also discussed, to which we shall come back later. In the end, we present results calculated using this nonchiral model together with what we obtain from a chirally invariant Lagrangian.

In Ref. [22], we discussed another interesting possibility of the density-driven π-η mixing in ANM. However, quantitatively, the mixing is found to be a higher order effect and does not affect the pion dispersion relations at the leading order in density. Hence in the present paper, we neglect π-η mixing.

The plan of the paper is as follows. In Sec. II we present the formalism, starting with PS coupling in Sec. II A. In Sec. II B we invoke nonlinear field transformation [25] and subsequently report results involving PV coupling. In Sec. III we present results using a recently developed chiral effective model in the context of the nuclear many-body problem [30,31]. Finally, Sec. IV presents the summary and conclusion. Detailed derivations for the Dirac part of the pion self-energy for PS and PV couplings have been relegated to Appendixes A and B, respectively.

II. FORMALISM

A. Model with pseudoscalar πN interaction

We start with the following interaction Lagrangian given by [25]

$$\begin{aligned}\mathcal{L} &= \bar{\Psi}(i\gamma_\mu\partial^\mu - M)\Psi - \tfrac{1}{2}g_\rho\bar{\Psi}\gamma_\mu\big(\vec{\tau}\cdot\vec{\Phi}_\rho^\mu\big)\Psi + g_s\bar{\Psi}\Phi_s\Psi \\ &\quad - g_\omega\bar{\Psi}\gamma_\mu\Phi_\omega^\mu\Psi - ig_\pi\bar{\Psi}\gamma_5\big(\vec{\tau}\cdot\vec{\Phi}_\pi\big)\Psi \\ &\quad + \tfrac{1}{2}\big(\partial_\mu\Phi_s\partial^\mu\Phi_s - m_s^2\Phi_s^2\big) + \tfrac{1}{2}\big(\partial_\mu\vec{\Phi}_\pi - g_\rho\vec{\Phi}_{\rho\mu}\times\vec{\Phi}_\pi\big) \\ &\quad \cdot\big(\partial^\mu\vec{\Phi}_\pi - g_\rho\vec{\Phi}_\rho^\mu\times\vec{\Phi}_\pi\big) - \tfrac{1}{2}m_\pi^2\vec{\Phi}_\pi^2 + \tfrac{1}{2}g_{\phi\pi}m_s\Phi_s\vec{\Phi}_\pi^2 \\ &\quad - \tfrac{1}{4}G_{\mu\nu}G^{\mu\nu} - \tfrac{1}{4}\vec{B}_{\mu\nu}\cdot\vec{B}^{\mu\nu} + \tfrac{1}{2}m_\omega^2\Phi_{\omega\mu}\Phi_\omega^\mu \\ &\quad + \tfrac{1}{2}m_\rho^2\vec{\Phi}_{\rho\mu}\cdot\vec{\Phi}_\rho^\mu, \end{aligned} \tag{1}$$

where

$$G_{\mu\nu} = \partial_\mu\Phi_{\omega\nu} - \partial_\nu\Phi_{\omega\mu}, \tag{2a}$$

$$\vec{B}_{\mu\nu} = \partial_\mu\vec{\Phi}_{\rho\nu} - \partial_\nu\vec{\Phi}_{\rho\mu} - g_\rho\vec{\Phi}_{\rho\mu}\times\vec{\Phi}_{\rho\nu}. \tag{2b}$$

Here, $\Psi, \vec{\Phi}_\pi, \Phi_s, \vec{\Phi}_\rho$, and Φ_ω represents the nucleon, pion, σ, ρ, and ω fields, respectively, and their masses are denoted by M, m_π, m_s, m_ρ, and m_ω. This model successfully reproduces the saturation properties of nuclear matter and yields accurate results for closed shell nuclei in the Dirac-Hartree approximation [32].

Note that in Eq. (1) the pion-nucleon dynamics is described by

$$\mathcal{L}^{\mathrm{PS}} = -ig_\pi\bar{\Psi}\gamma_5(\vec{\tau}\cdot\vec{\Phi}_\pi)\Psi, \tag{3}$$

where g_π is the pion-nucleon coupling constant with $\frac{g_\pi^2}{4\pi} = 12.6$ [33]. Besides this, the interaction Lagrangian of Eq. (1) also has another term involving the coupling of pions with the scalar meson given by

$$\mathcal{L}_s = \tfrac{1}{2}g_{\phi\pi}m_s\Phi_s\vec{\Phi}_\pi^2. \tag{4}$$

Here, $g_{\phi\pi}$ is the coupling constant of the scalar to pion field. The πN scattering amplitude would now involve both the nucleon and σ meson in the intermediate state, causing sensitive cancellation between the two, which gives a reasonable value for the s-wave scattering length [24] as mentioned before. At the self-energy level, Eqs. (3) and (4) will generate the exchange and the tadpole diagrams, as shown in Figs. 1(b) and 1(a), respectively.

First we consider the tadpole diagram, whose contribution to the self-energy is given by $\Sigma^{\mathrm{TC}} = -g_{\phi\pi}m_s\phi_0$, where $\phi_0 =$

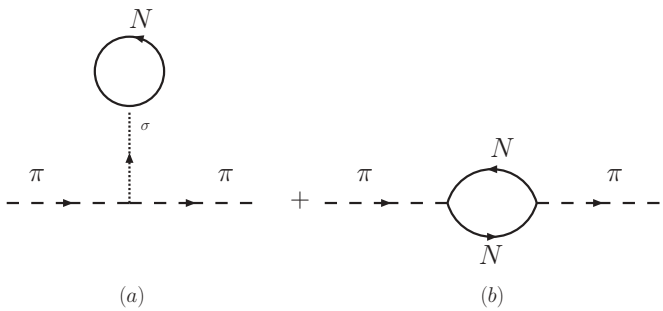

FIG. 1. Tadpole contribution to the pion self-energy.

$\frac{g_s}{m_s^2}\rho^s$ and $\rho^s = \rho_p^s + \rho_n^s$. Here $\rho_i^s (i = p, n)$ represents scalar density given by

$$\rho_i^s = \frac{M_i^*}{2\pi^2}\left[E_i^* k_i - M_i^{*2} \ln\left(\frac{E_i^* + k_i}{M_i^*}\right)\right]. \tag{5}$$

The effective nucleon mass M_i^* in Eq. (5) can be determined from the following self-consistent condition [34]:

$$M_i^* = M_i - \frac{g_s^2}{m_s^2}\left(\rho_p^s + \rho_n^s\right). \tag{6}$$

It is clear from Eq. (6) that $\Delta M^* = M_n - M_p = \Delta M$ as the nucleon masses are modified by the scalar mean field [34], which does not distinguish between n and p. Here, for the moment, we neglect explicit symmetry breaking (n-p mass difference), i.e., $M_p^* = M_n^* = M^*$.

Note that in the mean field theory (MFT), only Fig. 1(a), i.e., the tadpole diagram, contributes, while Fig. 1(b) is neglected. The origin of the tachyonic mode can now be easily understood. The pion mass in matter due to the tadpole is given by [24]

$$\begin{aligned} m_\pi^{*2} &= m_\pi^2 + \Sigma^{\mathrm{TC}} \\ &= m_\pi^2 - g_{\phi\pi} m_s \phi_0 \\ &= m_\pi^2 - \frac{g_{\phi\pi} g_s}{m_s}\left(\rho_n^s + \rho_p^s\right). \end{aligned} \tag{7}$$

The second term of the last equation is quite large even at densities far below ρ_0 density, viz., for $\rho \sim 0.1\rho_0$, $m_\pi^{*2} < 0$.

Figure 1(b) would involve various combinations of n and p depending upon the various charged states of pions, as shown in Fig. 2.

$$\Sigma^*(q) = -i\int \frac{d^4k}{(2\pi)^4}\mathrm{Tr}[\{i\Gamma(q)\} iG_i(k+q)\{i\Gamma(-q)\} iG_j(k)], \tag{8}$$

where the subscript $i(j)$ denotes either p (proton) or n (neutron). $\Gamma(q)$ is the vertex factor. $\Gamma = -i\gamma_5$ or $-i\frac{f_\pi}{m_\pi}\gamma_5\gamma_\mu q^\mu$ for the PS or PV coupling, respectively. Explicitly,

$$G_i(k) = G_i^F(k) + G_i^D(k), \tag{9}$$

where

$$G_i^F(k) = \frac{\not{k} + M_i^*}{k^2 - M_i^{*2} + i\zeta}, \tag{10a}$$

$$G_i^D(k) = \frac{i\pi(\not{k} + M_i^*)}{E_i^*}\delta(k_0 - E_i^*)\theta\left(k_i^F - |\mathbf{k}|\right). \tag{10b}$$

Here, $G_i^F(k)$ and $G_i^D(k)$ represent the free and density-dependent parts of the propagator. In Eq. (10), k is the nucleon momentum, k_i^F denotes the Fermi momentum, and M_i^* is the in-medium nucleon mass modified due to the scalar mean field [34]. From now on, we use k_p and k_n to denote the proton and neutron Fermi momenta, respectively. The nucleon energy is $E_i^* = \sqrt{M_i^{*2} + \mathbf{k}^2}$.

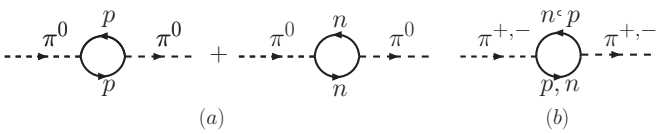

FIG. 2. One-loop self-energy diagrams for (a) π^0 and (b) $\pi^\pm$.

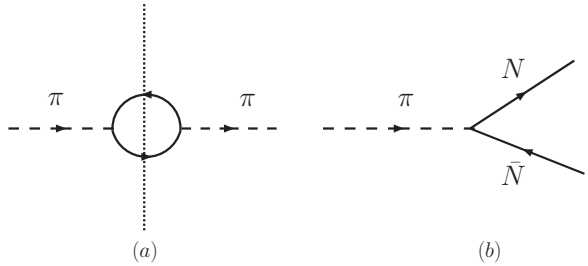

FIG. 3. Diagram (a) represents the cutting of the loop implied by the product of two δ functions, and (b) represents the decay of the pion into a nucleon-antinucleon pair.

Note that the total self-energy is given by $\Sigma^*_{\mathrm{total}}(q) = \Sigma^*(q) + \Sigma^{\mathrm{TC}}$. Using Eqs. (9) and (10), the expression for self-energy given in Eq. (8) takes the form

$$\begin{aligned} \Sigma^*(q) &= -ig^2\int \frac{d^4k}{(2\pi)^4}\mathbf{T} \\ &= \Sigma^{*\mathrm{FF}}(q) + \Sigma^{*(\mathrm{FD}+\mathrm{DF})}(q) + \Sigma^{*\mathrm{DD}}(q). \end{aligned} \tag{11}$$

Here g is g_π (f_π/m_π) for the PS (PV) coupling. For $\pi^\pm$ the coupling constant g_π (or f_π) gets replaced by $\sqrt{2}g_\pi$. The values of the coupling constants g_π and f_π are determined experimentally from πN and NN scattering data. $\mathbf{T}$ is the trace factor which consists of four parts:

$$\mathbf{T} = \mathbf{T}^{\mathrm{FF}} + \mathbf{T}^{\mathrm{FD}} + \mathbf{T}^{\mathrm{DF}} + \mathbf{T}^{\mathrm{DD}}. \tag{12}$$

Detailed expressions for $\mathbf{T}^{\mathrm{FF}}$, $\mathbf{T}^{\mathrm{FD}}$, and $\mathbf{T}^{\mathrm{DF}}$ will be discussed later. Here the term $\mathbf{T}^{\mathrm{DD}}$ contains the product of two δ functions $[G^D(k)G^D(k+q)]$, which puts both the loop nucleons on shell, implying the cut in the loop [Fig. 3(a)]. This means that the pion can decay into a nucleon-antinucleon [Fig. 3(b)] pair which happens only in the high momentum limit; i.e., $q > 2k_{p,n}$ and also $q_0 > 2E_{p,n}^F$, where $E_{p,n}^F$ is the Fermi energy for proton (or neutron). Under these conditions, only $\mathbf{T}^{\mathrm{DD}}$ contributes to the self-energy. But in the present calculation, we investigate only the low-momentum (of pion) collective excitations [35]. Therefore, $\mathbf{T}^{\mathrm{DD}}$ [i.e., $\Sigma^{*\mathrm{DD}}(q)$] is neglected.

Thus, the pion self-energy can now be written as

$$\Sigma^*(q) = -ig^2\int \frac{d^4k}{(2\pi)^4}[\mathbf{T}^{\mathrm{FF}} + (\mathbf{T}^{\mathrm{FD}} + \mathbf{T}^{\mathrm{DF}})]. \tag{13}$$

The self-energies for different charged states of pion are calculated using the one-loop diagram shown in the Fig. 2(b). The first term of Eq. (13) is same as the pion self-energy in vacuum with $M_i \to M_i^*$. This part is divergent.

$$\begin{aligned} \mathbf{T}_{\mathrm{PS}}^{\mathrm{FF}} &= 2\,\mathrm{Tr}[\gamma_5 iG^F(k)\gamma_5 iG^F(k+q)] \\ &= -8\left[\frac{M^{*2} - k\cdot(k+q)}{(k^2 - M^{*2})((k+q)^2 - M^{*2})}\right]. \end{aligned} \tag{14}$$

Here the factor 2 that appears in $\mathbf{T}_{\mathrm{PS}}^{\mathrm{FF}}$, i.e., in Eq. (14), follows from isospin symmetry for $M_n = M_p$. The FF part of self-energy for the PS coupling is calculated from Eq. (13) by

substituting $\mathbf{T}_{\rm PS}^{\rm FF}$, and it is denoted by $\Sigma_{\rm PS}^{*\rm FF}(q)$ as

$$\Sigma_{\rm PS}^{*\rm FF}(q) = 8ig_\pi^2 \int \frac{d^4k}{(2\pi)^4} \times \left[\frac{M^{*2} - k\cdot(k+q)}{(k^2 - M^{*2})((k+q)^2 - M^{*2})}\right]. \quad (15)$$

From Eq. (15) it is observed that $\Sigma_{\rm PS}^{*\rm FF}(q)$ is quadratically divergent. To eliminate these divergences, we need to renormalize $\Sigma_{\rm PS}^{*\rm FF}(q)$. Here we adopt the dimensional regularization technique [36–38] to regularize $\Sigma_{\rm PS}^{*\rm FF}(q)$ with the following results (details are discussed in Appendix A).

$$\begin{aligned}\Sigma_{\rm PS}^{*R}(q, m_\pi) &= \frac{g_\pi^2}{2\pi^2}\left[-3(M^2 - M^{*2}) + \left(q^2 - m_\pi^2\right)\left(\frac{1}{6} + \frac{M^2}{m_\pi^2}\right)\right. \\ &- 2M^{*2}\ln\left(\frac{M^*}{M}\right) + \frac{8M^2(M-M^*)^2}{\left(4M^2 - m_\pi^2\right)} \\ &- \frac{2M^{*2}\sqrt{4M^{*2} - q^2}}{q}\tan^{-1}\left(\frac{q}{\sqrt{4M^{*2} - q^2}}\right) \\ &+ \frac{2M^2\sqrt{4M^2 - m_\pi^2}}{m_\pi}\tan^{-1}\left(\frac{m_\pi}{\sqrt{4M^2 - m_\pi^2}}\right) \\ &+ \left((M^2 - M^{*2}) + \frac{m_\pi^2(M-M^*)^2}{(4M^2 - m_\pi^2)} + \frac{M^2}{m_\pi^2}\left(q^2 - m_\pi^2\right)\right) \\ &\times \frac{8M^2}{m_\pi\sqrt{4M^2 - m_\pi^2}}\tan^{-1}\left(\frac{m_\pi}{\sqrt{4M^2 - m_\pi^2}}\right) \\ &\left. + \int_0^1 dx\, 3x(1-x)q^2\ln\left(\frac{M^{*2} - q^2x(1-x)}{M^2 - m_\pi^2 x(1-x)}\right)\right] \quad (16)\end{aligned}$$

It is found that the result given in Eq. (16) is finite and no divergences appear further. In the appropriate kinematic regime, it might generate the imaginary part

$$\begin{aligned}{\rm Im}\Sigma_{\rm PS}^{*\rm FF}(q) &= -\frac{g_\pi^2}{2\pi^2}\int_0^1 dx\,(M^{*2} - 3q^2x(1-x)) \\ &\times {\rm Im}[\ln(M^{*2} - q^2x(1-x) - i\eta)] \\ &= -\frac{g_\pi^2}{4\pi}[q\sqrt{q^2 - 4M^{*2}}]\,\theta(q^2 - 4M^{*2}). \quad (17)\end{aligned}$$

If we consider that $(M^* - M)$ is small enough, then the term $\ln[(M^{*2} - q^2x(1-x))/(M^2 - m_\pi^2 x(1-x))]$ of Eq. (16) can be approximated to $2\ln(M^*/M)$, and the last term of Eq. (16) can be easily evaluated to give

$$\Sigma_{\rm PS}^{*R}(q, m_\pi) \simeq -\tilde{\mathcal{C}} + \tilde{\mathcal{D}}q^2, \quad (18)$$

where

$$\left.\begin{aligned}\tilde{\mathcal{C}} &= \tfrac{g_\pi^2}{2\pi^2}\left[3(2M^2 - M^{*2}) + 2M^{*2}\ln\left(\tfrac{M^*}{M}\right)\right], \\ \tilde{\mathcal{D}} &= \tfrac{g_\pi^2}{2\pi^2}\left[3\left(\tfrac{M}{m_\pi}\right)^2\right].\end{aligned}\right\} \quad (19)$$

The trace of the (FD+DF) part is for π^0,

$$\begin{aligned}&T_{\rm PS}^{\rm FD} + T_{\rm PS}^{\rm DF} \\ &= {\rm Tr}\left[\gamma_5 G_p^F(k+q)\gamma_5 G_p^D(k) + \gamma_5 G_p^D(k+q)\gamma_5 G_p^F(k)\right] \\ &\quad + [p \to n], \quad (20)\end{aligned}$$

and for $\pi^{+(-)}$,

$$\begin{aligned}T_{\rm PS}^{\rm FD} + T_{\rm PS}^{\rm DF} &= {\rm Tr}\left[\gamma_5 G_{p(n)}^F(k+q)\gamma_5 G_{n(p)}^D(k)\right. \\ &\left. + \gamma_5 G_{p(n)}^D(k+q)\gamma_5 G_{n(p)}^F(k)\right]. \quad (21)\end{aligned}$$

The (FD+DF) part of the self-energy for π^0 and $\pi^\pm$ can be written as

$$\Sigma_{\rm PS}^{*0(\rm FD+DF)}(q) = -8g_\pi^2\int\frac{d^3k}{(2\pi)^3E^*}\mathbf{A}_{\rm PS}, \quad (22)$$

$$\begin{aligned}\Sigma_{\rm PS}^{*\pm(\rm FD+DF)}(q) &= -8g_\pi^2\int\frac{d^3k}{(2\pi)^3E^*}[\mathbf{A}_{\rm PS} \mp \mathbf{B}_{\rm PS}] \\ &= \Sigma_{\rm PS}^{*0(\rm FD+DF)}(q) \mp \delta\Sigma_{\rm PS}^{*(\rm FD+DF)}(q), \quad (23)\end{aligned}$$

where

$$\mathbf{A}_{\rm PS} = \left[\frac{(k\cdot q)^2}{q^4 - 4(k\cdot q)^2}\right](\theta_p + \theta_n), \quad (24)$$

$$\mathbf{B}_{\rm PS} = \frac{1}{2}\left[\frac{q^2(k\cdot q)}{q^4 - 4(k\cdot q)^2}\right](\theta_p - \theta_n), \quad (25)$$

with $\theta_{p,n} = \theta(k_{p,n} - |\mathbf{k}|)$. We restrict ourselves in the long wavelength limit, i.e., when the pion momentum $\mathbf{q}$ is smaller than the Fermi momentum $k_{p,n}$ of the system, where the many-body effects manifest strongly. In this case, particle propagation can be understood in terms of collective excitation [35] of the system, which permits analytical solutions of the dispersion relations [35,39]. But in the short wavelength limit, i.e., when $\mathbf{q}$ is much larger than $k_{p,n}$, particle dispersion approaches that of the free propagation. Note that for SNM, $\mathbf{B}_{\rm PS} = 0$, implying that $\Sigma_{\rm PS}^{*\pm(\rm FD+DF)} = \Sigma_{\rm PS}^{*0(\rm FD+DF)}$.

In the long wavelength limit, we neglect the term q^4 compared to the term $4(k\cdot q)^2$ from the denominator of both $\mathbf{A}_{\rm PS}$ and $\mathbf{B}_{\rm PS}$ in Eqs. (24) and (25). Explicitly, after a straightforward calculation, we get

$$\begin{aligned}\Sigma_{\rm PS}^{*0(\rm FD+DF)}(q) &= \frac{g_\pi^2}{2\pi^2}\left[\left(k_pE_p^* - \frac{1}{2}M^{*2}\ln\left|\frac{1+v_p}{1-v_p}\right|\right)\right. \\ &\left. + \left(k_nE_n^* - \frac{1}{2}M^{*2}\ln\left|\frac{1+v_n}{1-v_n}\right|\right)\right], \quad (26)\end{aligned}$$

and

$$\begin{aligned}&\delta\Sigma_{\rm PS}^{*(\rm FD+DF)}(q) \\ &= \frac{g_\pi^2}{2\pi^2}\left[\frac{1}{2}E_p^*\ln\left|\frac{c_0+v_p}{c_0-v_p}\right| - \frac{M^*}{\sqrt{c_0^2-1}}\tan^{-1}\right. \\ &\times\left.\left(\frac{k_p\sqrt{c_0^2-1}}{c_0M^*}\right)\right]\frac{q^2}{|\mathbf{q}|} - \frac{g_\pi^2}{2\pi^2}\left[\frac{1}{2}E_n^*\ln\left|\frac{c_0+v_n}{c_0-v_n}\right|\right. \\ &\left. - \frac{M^*}{\sqrt{c_0^2-1}}\tan^{-1}\left(\frac{k_n\sqrt{c_0^2-1}}{c_0M^*}\right)\right]\frac{q^2}{|\mathbf{q}|}, \quad (27)\end{aligned}$$

where $v_{p,n} = k_{p,n}/E^*_{p,n}$, $E^*_{p,n} = \sqrt{M^{*2} + k^2_{p,n}}$, and $c_0 = q_0/|\mathbf{q}|$. The approximate results of Eqs. (26) and (27) are given below.

$$\Sigma^{*0(\mathrm{FD+DF})}_{\mathrm{PS}}(q) \simeq -\tilde{\mathcal{A}} - \tilde{\mathcal{B}} - \tilde{\mathcal{F}} + \tilde{\mathcal{G}}, \tag{28}$$

$$\delta\Sigma^{*(\mathrm{FD+DF})}_{\mathrm{PS}}(q) \simeq \tilde{\mathcal{E}}\frac{q^2}{q_0}, \tag{29}$$

where

$$\left.\begin{aligned}
\tilde{\mathcal{A}} &= \tfrac{g_\pi^2}{2\pi^2}\left[\tfrac{1}{3}\left(\tfrac{k_p^3}{E_p^{*3}} + \tfrac{k_n^3}{E_n^{*3}}\right)\right]M^{*2},\\
\tilde{\mathcal{B}} &= \tfrac{g_\pi^2}{2\pi^2}\left[\tfrac{1}{5}\left(\tfrac{k_p^5}{E_p^{*5}} + \tfrac{k_n^5}{E_n^{*5}}\right)\right]M^{*2},\\
\tilde{\mathcal{F}} &= \tfrac{g_\pi^2}{2\pi^2}\left[\left(\tfrac{k_p}{E_p^{*}} + \tfrac{k_n}{E_n^{*}}\right)\right]M^{*2},\\
\tilde{\mathcal{G}} &= \tfrac{g_\pi^2}{2\pi^2}\left[k_p E_p^* + k_n E_n^*\right],\\
\tilde{\mathcal{E}} &= \tfrac{g_\pi^2}{2\pi^2}\left[\tfrac{1}{3}\left(\tfrac{k_p^3}{M^{*2}} - \tfrac{k_n^3}{M^{*2}}\right)\right].
\end{aligned}\right\} \tag{30}$$

The self-energy for PS coupling is

$$\Sigma^{*0,\pm}_{\mathrm{PS}}(q) = \Sigma^{*R}_{\mathrm{PS}}(q, m_\pi) + \Sigma^{*0,\pm(\mathrm{FD+DF})}_{\mathrm{PS}}(q). \tag{31}$$

The dispersion relations are found by solving the Dyson-Schwinger equation and obtaining

$$q^2 - m^2_{\pi^{0,\pm}} - (\Sigma^{*0,\pm}(q) + \Sigma^{\mathrm{TC}}) = 0. \tag{32}$$

Here $m_{\pi^{0,\pm}}$ are the masses of π^0 and $\pi^\pm$. The dispersion relations without the effect of the Dirac sea for $\pi^{0,\pm}$ are

$$q_0^2 \simeq m^{*2}_{\pi^{0,\pm}} + \mathbf{q}^2. \tag{33}$$

The effective masses without the Dirac sea are

$$\left.\begin{aligned}
m^{*2}_{\pi^0} &\simeq \left[\Omega_{\mathrm{PS}} + \Sigma^{\mathrm{TC}} + m^2_{\pi^0}\right],\\
m^{*2}_{\pi^\pm} &\simeq \left[\frac{\Omega_{\mathrm{PS}} + \Sigma^{\mathrm{TC}} + m^2_{\pi^\pm}}{1 \mp \delta\Omega_{\mathrm{PS}}}\right],
\end{aligned}\right\} \tag{34}$$

where

$$\left.\begin{aligned}
\Omega_{\mathrm{PS}} &= \tilde{\mathcal{G}} - \tilde{\mathcal{A}} - \tilde{\mathcal{B}} - \tilde{\mathcal{F}},\\
\delta\Omega_{\mathrm{PS}} &= \frac{\tilde{\mathcal{E}}}{\sqrt{\Omega_{\mathrm{PS}} + \Sigma^{\mathrm{TC}} + m^2_{\pi^\pm}}}.
\end{aligned}\right\} \tag{35}$$

Now we present the dispersion relations for $\pi^{0,\pm}$ with the effect of the Dirac sea:

$$q_0^2 \simeq m^{*2}_{\pi^{0,\pm}} + \mathbf{q}^2 \tag{36}$$

The effective masses ($m^{*2}_{\pi^{0,\pm}}$) with the Dirac sea for different charged states of pion are given by

$$\left.\begin{aligned}
m^{*2}_{\pi^0} &\simeq \left[\left(\Lambda_{\mathrm{PS}} - m^2_{\pi^0}\right)/\tilde{\mathcal{D}}\right],\\
m^{*2}_{\pi^\pm} &\simeq \left[\frac{\left(\Lambda_{\mathrm{PS}} - m^2_{\pi^\pm}\right)}{(1 \mp \delta\Lambda_{\mathrm{PS}})\tilde{\mathcal{D}}}\right],
\end{aligned}\right\} \tag{37}$$

where

$$\left.\begin{aligned}
\Lambda_{\mathrm{PS}} &= \tilde{\mathcal{C}} - \Omega_{\mathrm{PS}} - \Sigma^{\mathrm{TC}},\\
\delta\Lambda_{\mathrm{PS}} &= \frac{\tilde{\mathcal{E}}}{\sqrt{(\Lambda_{\mathrm{PS}} - m^2_{\pi^\pm})\tilde{\mathcal{D}}}}.
\end{aligned}\right\} \tag{38}$$

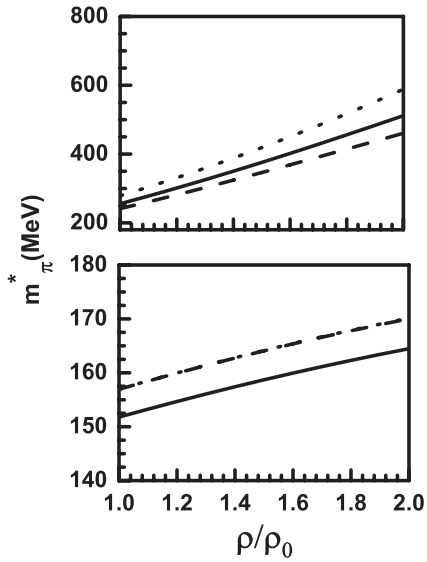

FIG. 4. Nuclear density (ρ) dependent effective pion masses for PS coupling at $\alpha = 0.2$. The dotted, dashed, and solid curves representing π^-, π^+, and π^0 without (upper panel) and with (lower panel) the Dirac sea effect.

In the PS coupling, the asymmetry-driven mass splitting is of $\mathcal{O}(k^3_{p(n)}/M^{*2})$. The terms $\delta\Lambda_{\mathrm{PS}}$ and $\delta\Omega_{\mathrm{PS}}$ are nonvanishing in ANM and responsible for the pion mass splitting.

In Figs. 4 and 5 we present the density ρ and asymmetry parameter α dependent effective masses for the various charged states of pion. In the top panel, we present the results without vacuum correction (Dirac sea). Here we include both the tadpole and n-n loop.

It is evident that the inclusion of Fig. 1(b) removes the tachyonic mode but gives rise to effective pion masses that are

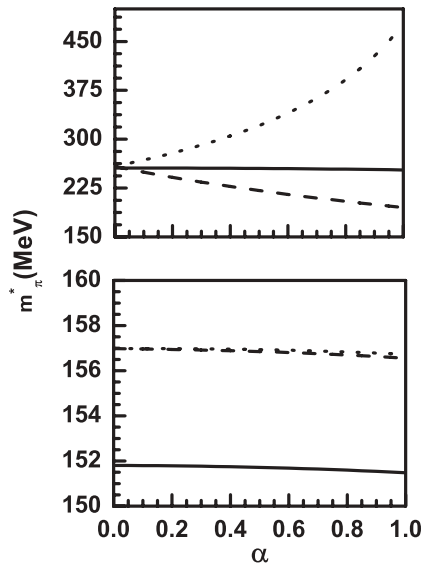

FIG. 5. Asymmetry parameter (α) dependent effective pion masses for π^0 (solid curve), π^+ (dashed curve), and π^- (dotted curve) in ANM at NNM density for PS coupling. The upper and lower panels, respectively, represent effective pion masses without and with vacuum correction.

TABLE I. Effective pion masses including the tadpole contribution to the self-energy in PS coupling. Kapusta corresponds to Ref. [24] and BDM corresponds to the present calculation.

	$m^*2_{\pi^0}$	$m^*2_{\pi^\pm}$
MFT	$m^2_{\pi^0} + \Sigma^{\rm TC}$	$m^2_{\pi^\pm} + \Sigma^{\rm TC}$
Kapusta	$\Omega_{\rm PS} + (\Sigma^{\rm TC} + m^2_{\pi^0})$	$\frac{\Omega_{\rm PS}+(\Sigma^{\rm TC}+m^2_{\pi^\pm})}{1\mp\delta\Omega_{\rm PS}}$
BDM	$[\tilde{\mathcal{C}} - (\Omega_{\rm PS} + \Sigma^{\rm TC} + m^2_{\pi^0})]/\tilde{\mathcal{D}}$	$\frac{\tilde{\mathcal{C}}-(\Omega_{\rm PS}+\Sigma^{\rm TC}+m^2_{\pi^\pm})}{(1\mp\delta\Lambda_{\rm PS})\tilde{\mathcal{D}}}$

unrealistically large, as discussed by Kapusta [24] as shown in the top panel of Fig. 4.

Note that the inclusion of the vacuum part reduces the effective pion masses and gives reasonable value for the density-dependent pion masses in matter at NNM density. The reason for this could be understood from Table I, which enumerates expressions for the effective pion masses that we obtain in three different cases. The top row represents effective pion masses for the case considered in Ref. [23] which gives rise to the tachyonic mode, the second row corresponds to the case discussed by Kapusta [24], and the last row presents results of the present work, designated as BDM. The presence of the additional term $\tilde{\mathcal{D}}$ somewhat tames the dispersion curve bringing the masses down compared to those in Ref. [24]. This can be noted that at the MFT level, $\Sigma^{\rm TC}$ involves the sum of the scalar densities ρ^s_n and ρ^s_p. Therefore, in MFT, as expected, the masses are insensitive to the asymmetry parameter α.

For Pb-like nuclei ($\alpha = 0.2$), $\Delta m_{\pi^0} = 16.8$, $\Delta m_{\pi^+} = 17.37$, and $\Delta m_{\pi^-} = 17.41$ MeV with vacuum correction.

The dispersion relation for various charged states of pion are shown in the Fig. 6, where upper and lower panels present the dispersion curves without and with the Dirac sea including the tadpole contribution. In the presence of the Dirac sea, π^+ and π^- dispersion curves are indistinguishable.

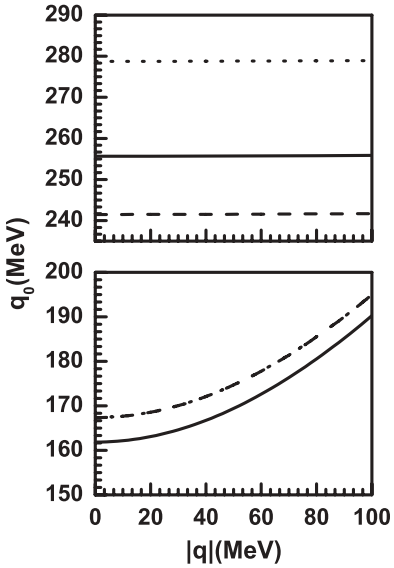

FIG. 6. Dispersion relations of π^0 (solid curve), π^+ (dashed curve), and π^- (dotted curve) for PS coupling at $\rho = 0.17$ fm^{-3} and $\alpha = 0.2$. The upper and lower panels represent pion dispersions without and with the Dirac sea.

B. Renormalizable model with pseudovector πN coupling

To obtain the pseudovector representation from the starting Lagrangian given by Eq. (1), one gives the following nonlinear chiral transformation [25]:

$$\Psi = \left[\frac{1 - i\gamma_5\vec{\tau}\cdot\vec{\xi}}{\sqrt{1+\vec{\xi}^2}}\right]\Psi', \tag{39a}$$

$$\vec{\xi} = \left(\frac{f_\pi}{m_\pi}\right)\vec{\Phi}'_\pi = g_\pi\vec{\Phi}_\pi \Big/ \left[M - g_s\Phi_s + \sqrt{(M-g_s\Phi_s)^2 + g_\pi^2\vec{\Phi}^2_\pi}\right], \tag{39b}$$

$$g_s\Phi'_s = M - \sqrt{(M-g_s\Phi_s)^2 + g_\pi^2\vec{\Phi}^2_\pi}. \tag{39c}$$

The last two equations (39b) and (39c) are used to express the old fields Φ_s and $\vec{\Phi}_\pi$ in terms of new fields Φ'_s and $\vec{\Phi}'_\pi$.

$$\vec{\Phi}_\pi = \left[\frac{1 - 2(f_\pi/m_\pi)\Phi'_s}{1 + (f_\pi/m_\pi)^2\vec{\Phi}'^2_\pi}\right]\vec{\Phi}'_\pi, \tag{40a}$$

$$\Phi_s = \frac{\left(1 - (f_\pi/m_\pi)^2\vec{\Phi}'^2_\pi\right)\Phi'_s + (g_\pi/g_s)(f_\pi/m_\pi)\vec{\Phi}'^2_\pi}{1 + (f_\pi/m_\pi)^2\vec{\Phi}'^2_\pi}. \tag{40b}$$

The transformed Lagrangian is

$$\begin{aligned}
\mathcal{L}' = {} & \bar{\Psi}'(i\gamma_\mu\partial^\mu - M)\Psi' - \frac{1}{2}g_\rho\bar{\Psi}'\gamma_\mu\left(\vec{\tau}\cdot\vec{\Phi}^\mu_\rho\right)\Psi' + g_s\bar{\Psi}'\Phi'_s\Psi' \\
& - g_\omega\bar{\Psi}'\gamma_\mu\Phi^\mu_\rho\Psi' + \frac{1}{2}\left(\partial_\mu\Phi_s\partial^\mu\Phi_s - m_s^2\Phi_s^2\right) \\
& + \frac{1}{2}(\partial_\mu\vec{\Phi}_\pi - g_\rho\vec{\Phi}_{\rho\mu}\times\vec{\Phi}_\pi)\cdot\left(\partial^\mu\vec{\Phi}_\pi - g_\rho\vec{\Phi}^\mu_\rho\times\vec{\Phi}_\pi\right) \\
& - \frac{1}{2}m_\pi^2\vec{\Phi}^2_\pi + \frac{1}{2}g_{\phi\pi}m_s\Phi_s\vec{\Phi}^2_\pi - \frac{1}{4}G_{\mu\nu}G^{\mu\nu} \\
& - \frac{1}{4}\vec{B}_{\mu\nu}\cdot\vec{B}^{\mu\nu} + \frac{1}{2}m_\omega^2\Phi_{\omega\mu}\Phi^\mu_\omega + \frac{1}{2}m_\rho^2\vec{\Phi}_{\rho\mu}\cdot\vec{\Phi}^\mu_\rho \\
& - \frac{(f_\pi/m_\pi)^2}{1 + (f_\pi/m_\pi)^2\vec{\Phi}'^2_\pi}\bar{\Psi}'\gamma_\mu\left(\vec{\tau}\cdot\vec{\Phi}'_\pi\right) \\
& \times\left(\partial^\mu\vec{\Phi}'_\pi - g_\rho\vec{\Phi}^\mu_\rho\times\vec{\Phi}'_\pi\right)\Psi' - \frac{(f_\pi/m_\pi)}{1 + (f_\pi/m_\pi)^2\vec{\Phi}'^2_\pi} \\
& \times\bar{\Psi}'\gamma_5\gamma_\mu\vec{\tau}\cdot\left(\partial^\mu\vec{\Phi}'_\pi - g_\rho\vec{\Phi}^\mu_\rho\times\vec{\Phi}'_\pi\right)\Psi'.
\end{aligned} \tag{41}$$

We see from Eq. (41) that the π-N PS coupling has disappeared and instead the pion-nucleon dynamics is now governed by the last term of the above-mentioned equation. At the leading order, one obtains the usual PV coupling represented by

$$\mathcal{L}^{\rm PV} = -\frac{f_\pi}{m_\pi}\bar{\Psi}'\gamma_5\gamma^\mu\partial_\mu(\vec{\tau}\cdot\vec{\Phi}'_\pi)\Psi'. \tag{42}$$

Here f_π is the pseudovector coupling constant and $\frac{f_\pi^2}{4\pi} = 0.08$ [40]. First we discuss the FF part, where the trace factor is given by

$$\begin{aligned}\mathbf{T}_{\rm PV}^{\rm FF} &= -2{\rm Tr}[\gamma_5\gamma^\mu q_\mu i G^F(k)\gamma_5\gamma^\nu q_\nu i G^F(k+q)] \\ &= -8\left[\frac{M^{*2}q^2 + k\cdot(k+q)q^2 - 2(k\cdot q)(k+q)\cdot q}{(k^2-M^{*2})((k+q)^2-M^{*2})}\right].\end{aligned} \tag{43}$$

Now the FF part of the self-energy for PV coupling is denoted by $\Sigma_{\rm PV}^{*\rm FF}(q)$. From Eqs. (13) and(43) we get

$$\begin{aligned}\Sigma_{\rm PV}^{*\rm FF}(q) &= 8i\left(\frac{f_\pi}{m_\pi}\right)^2\int\frac{d^4k}{(2\pi)^4} \\ &\times\left[\frac{M^{*2}q^2 + k\cdot(k+q)q^2 - 2(k\cdot q)(k+q)\cdot q}{(k^2-M^{*2})((k+q)^2-M^{*2})}\right].\end{aligned} \tag{44}$$

Direct power counting shows that the term $\Sigma_{\rm PV}^{*\rm FF}(q)$ is divergent. The appropriate renormalization scheme for the present model has been developed in Ref. [25]. We first consider a simple subtraction scheme (described in Appendix B) to obtain

$$\begin{aligned}\Sigma_{\rm PV}^{*R}(q) &= \frac{q^2}{2\pi^2}\left(\frac{f_\pi}{m_\pi}\right)^2 \\ &\times\left[2M^{*2}\int_0^1 dx\,\ln\left(\frac{M^{*2}-q^2x(1-x)}{M^{*2}-m_\pi^2x(1-x)}\right)\right].\end{aligned} \tag{45}$$

Now $\Sigma_{\rm PV}^{*R}(q)$ can be approximated to

$$\Sigma_{\rm PV}^{*R}(q) \simeq \mathcal{C}q^2 - \mathcal{D}q^4, \tag{46}$$

where

$$\left.\begin{aligned}\mathcal{C} &= \left(\tfrac{f_\pi M^*}{m_\pi\pi}\right)^2\left[\tfrac{m_\pi^2}{6M^{*2}}\right], \\ \mathcal{D} &= \left(\tfrac{f_\pi M^*}{m_\pi\pi}\right)^2\left[\tfrac{1}{6M^{*2}}\right].\end{aligned}\right\} \tag{47}$$

On the other hand, borrowing results from Ref. [25], one has

$$\Sigma_{\rm PV}^{*R}(q) \simeq \mathcal{C}' + \mathcal{D}'q^2, \tag{48}$$

where

$$\left.\begin{aligned}\mathcal{C}' &= \left(\tfrac{f_\pi}{m_\pi\pi}\right)^2\left[\tfrac{4}{3}M(M-M^*)m_\pi^2\right], \\ \mathcal{D}' &= \left(\tfrac{f_\pi}{m_\pi\pi}\right)^2\left[2M^{*2}\ln(M^*/M)\right].\end{aligned}\right\} \tag{49}$$

It might be mentioned that although $\mathcal{C}, D$ are different from $\mathcal{C}', D'$, their effects on the effective pion masses and corresponding dispersion relations are found to be marginal, as we will discuss later.

The FF part can also develop an imaginary part as given by

$$\begin{aligned}{\rm Im}\Sigma_{\rm PV}^{*\rm FF}(q) &= -\left(\frac{f_\pi}{m_\pi}\right)^2 \\ &\times\left[\frac{q}{\pi}2M^{*2}\sqrt{q^2-4M^{*2}}\right]\theta(q^2-4M^{*2}).\end{aligned} \tag{50}$$

It is observed from Eq. (50) that ${\rm Im}\Sigma_{\rm PV}^{*\rm FF}(q)$ is nonvanishing only if $q^2 > 4M^{*2}$.

The trace of the (FD+DF) part for π^0 is

$$\begin{aligned}T_{\rm PV}^{\rm FD} + T_{\rm PV}^{\rm DF} &= {\rm Tr}\left[\gamma_5\not{q}G_p^F(k+q)\gamma_5\not{q}G_p^D(k)\right. \\ &\left.+\gamma_5\not{q}G_p^D(k+q)\gamma_5\not{q}G_p^F(k)\right] + [p\to n],\end{aligned} \tag{51}$$

and for $\pi^{+(-)}$,

$$\begin{aligned}T_{\rm PV}^{\rm FD} + T_{\rm PV}^{\rm DF} &= {\rm Tr}\left[\gamma_5\not{q}G_{p(n)}^F(k+q)\gamma_5\not{q}G_{n(p)}^D(k)\right. \\ &\left.+\gamma_5\not{q}G_{p(n)}^D(k+q)\gamma_5\not{q}G_{n(p)}^F(k)\right].\end{aligned} \tag{52}$$

In pure neutron (or proton) matter, one of the terms of Eq. (52), viz., $G_{p(n)}^D = 0$ for the charged pion states. The same argument holds true for the neutral pion, where only two terms would contribute, which can be observed from Eq. (51). For pure neutron (or proton) matter, $p(n)$ appears as the intermediate state. Now the (FD+DF) part of the self-energy for π^0 and $\pi^\pm$ can be written as

$$\Sigma_{\rm PV}^{*0({\rm FD+DF})}(q) = -8\left(\frac{f_\pi}{m_\pi}\right)^2\int\frac{d^3k}{(2\pi)^3E^*}\mathbf{A}_{\rm PV}, \tag{53}$$

$$\begin{aligned}\Sigma_{\rm PV}^{*\pm({\rm FD+DF})}(q) &= -8\left(\frac{f_\pi}{m_\pi}\right)^2\int\frac{d^3k}{(2\pi)^3E^*}[\mathbf{A}_{\rm PV}\mp\mathbf{B}_{\rm PV}] \\ &= \Sigma_{\rm PV}^{*0({\rm FD+DF})}(q) \mp \delta\Sigma_{\rm PV}^{*({\rm FD+DF})}(q),\end{aligned} \tag{54}$$

where

$$\mathbf{A}_{\rm PV} = \left[\frac{M^{*2}q^4}{q^4-4(k\cdot q)^2}\right](\theta_p+\theta_n), \tag{55}$$

$$\mathbf{B}_{\rm PV} = \frac{1}{2}\left[1+\frac{4M^{*2}q^2}{q^4-4(k\cdot q)^2}\right](k\cdot q)(\theta_p-\theta_n). \tag{56}$$

In the long wavelength limit considering collective excitations near the Fermi surface, the (FD+DF) part of the pion self-energy can be evaluated analytically. In this case, we can neglect the term q^4 compared to the term $4(k\cdot q)^2$ from the denominator of $\mathbf{A}_{\rm PV}$ and $\mathbf{B}_{\rm PV}$ in Eqs. (55) and (56). This is called the hard nucleon loop (HNL) approximation [39]. Explicitly, after a straight-forward calculation, we get

$$\begin{aligned}&\Sigma_{\rm PV}^{*0({\rm FD+DF})}(q) \\ &= \frac{1}{2}\left(\frac{f_\pi M^*}{m_\pi\pi}\right)^2\left[\left(\ln\left|\frac{1+v_p}{1-v_p}\right| - c_0\ln\left|\frac{c_0+v_p}{c_0-v_p}\right|\right)\right. \\ &\left.+\left(\ln\left|\frac{1+v_n}{1-v_n}\right| - c_0\ln\left|\frac{c_0+v_n}{c_0-v_n}\right|\right)\right],\end{aligned} \tag{57}$$

and

$$\begin{aligned}&\delta\Sigma_{\rm PV}^{*({\rm FD+DF})}(q) \\ &= \left(\frac{f_\pi}{m_\pi\pi}\right)^2\left[\frac{2}{3}k_p^3q_0 - \frac{M^{*2}q^2}{|\mathbf{q}|}\left(E_p^*\ln\left|\frac{c_0+v_p}{c_0-v_p}\right|\right.\right. \\ &\left.\left.-\frac{2M^*}{\sqrt{c_0^2-1}}\tan^{-1}\frac{k_p\sqrt{c_0^2-1}}{c_0M^*}\right)\right] - \left(\frac{f_\pi}{m_\pi\pi}\right)^2\end{aligned}$$

$$\times \left[\frac{2}{3} k_n^3 q_0 - \frac{M^{*2} q^2}{|\mathbf{q}|} \left(E_n^* \ln \left| \frac{c_0 + v_n}{c_0 - v_n} \right| - \frac{2M^*}{\sqrt{c_0^2 - 1}} \tan^{-1} \frac{k_n \sqrt{c_0^2 - 1}}{c_0 M^*} \right) \right]. \quad (58)$$

The approximate results of Eqs. (57) and (58) are

$$\Sigma_{\rm PV}^{*0({\rm FD+DF})}(q) \simeq \mathcal{A} \frac{q^4}{q_0^2} + \mathcal{B} q^2, \quad (59)$$

$$\delta\Sigma_{\rm PV}^{*({\rm FD+DF})}(q) \simeq \mathcal{E} q_0, \quad (60)$$

where

$$\left.\begin{aligned} \mathcal{A} &= \left(\frac{f_\pi M^*}{m_\pi \pi}\right)^2 \left[\frac{1}{3}\left(\frac{k_p^3}{E_p^{*3}} + \frac{k_n^3}{E_n^{*3}}\right)\right], \\ \mathcal{B} &= \left(\frac{f_\pi M^*}{m_\pi \pi}\right)^2 \left[\frac{1}{5}\left(\frac{k_p^5}{E_p^{*5}} + \frac{k_n^5}{E_n^{*5}}\right)\right], \\ \mathcal{E} &= \left(\frac{f_\pi M^*}{m_\pi \pi}\right)^2 \left[\frac{2}{5}\left(\frac{k_p^5}{M^{*4}} - \frac{k_n^5}{M^{*4}}\right)\right]. \end{aligned}\right\} \quad (61)$$

The total pion self-energy for PV coupling is

$$\Sigma_{\rm PV}^{*0,\pm}(q) = \Sigma_{\rm PV}^{*R}(q) + \Sigma_{\rm PV}^{*0,\pm({\rm FD+DF})}(q). \quad (62)$$

The approximate dispersion relations and the effective pion masses of different charged states in ANM without and with the Dirac sea effect are presented below.

The dispersion relations for $\pi^{0,\pm}$ without the effect of the Dirac sea are

$$q_0^2 \simeq m_{\pi^{0,\pm}}^{*2} + \gamma_{\pi\pi} \mathbf{q}^2 + \left[\frac{\gamma_{\pi\pi}^2}{4} + \alpha_{\pi\pi}\right] \frac{\mathbf{q}^4}{m_{\pi^{0,\pm}}^{*2}}, \quad (63)$$

where $m_{\pi^{0,\pm}}^{*2}$ is the effective pion masses without the Dirac sea effect, that is,

$$m_{\pi^0}^{*2} \simeq \frac{m_{\pi^0}^2}{1 - \Omega_{\rm PV}} \quad \text{and} \quad m_{\pi^\pm}^{*2} \simeq \frac{m_{\pi^\pm}^2}{1 - (\Omega_{\rm PV} \pm \delta\Omega_{\rm PV})}, \quad (64)$$

where

$$\left.\begin{aligned} \Omega_{\rm PV} &= \mathcal{A} + B, \\ \delta\Omega_{\rm PV} &= \frac{\mathcal{E}}{m_{\pi^\pm}}, \\ \gamma_{\pi\pi} &= 1 - \frac{\Omega_{\rm PV}}{1-\Omega_{\rm PV}} + \frac{\mathcal{B}}{1-\Omega_{\rm PV}}, \\ \alpha_{\pi\pi} &= \frac{\mathcal{A}}{1-\Omega_{\rm PV}}. \end{aligned}\right\} \quad (65)$$

These results are the same as that of Ref. [22] with some notational difference such as $\Omega_{\rm PV} \to \Omega_{\pi\pi}^2$, $\delta\Omega_{\rm PV} \to \delta\Omega_{\pi\pi}^2$, $\Omega_{\rm PV}/(1-\Omega_{\rm PV}) \to \chi_{\pi\pi}$, and $\mathcal{B}/(1-\Omega_{\rm PV}) \to \beta_{\pi\pi}$. In Eqs. (67) and (64), $\delta\Lambda_{\rm PV}$ and $\delta\Omega_{\rm PV}$ are responsible for the asymmetry parameter ($\alpha = \frac{\rho_n - \rho_p}{\rho_n + \rho_p}$) dependent mass splitting, where ρ_n and ρ_p are the neutron and proton density, respectively. Clearly for SNM, $\delta\Lambda_{\rm PV}$ and $\delta\Omega_{\rm PV}$ vanish.

The dispersion relations for $\pi^{0,\pm}$ including the effect of the Dirac sea are given by

$$q_0^2 \simeq m_{\pi^{0,\pm}}^{*2} + \left[\gamma_{\pi\pi} + 2 m_{\pi^{0,\pm}}^{*2} \delta_{\pi\pi}\right] \mathbf{q}^2 + \left[\frac{\gamma_{\pi\pi}^2}{4} + \alpha_{\pi\pi} - \delta_{\pi\pi}\left(m_{\pi^{0,\pm}}^{*2} - 2\gamma_{\pi\pi}\right)\right] \frac{\mathbf{q}^4}{m_{\pi^{0,\pm}}^{*2}}. \quad (66)$$

The effective masses m_π^* of different charged states of pion are found from Eq. (66) in the limit $|\mathbf{q}| = 0$, i.e.,

$$m_{\pi^0}^{*2} \simeq \frac{m_{\pi^0}^2}{1 - \Lambda_{\rm PV}} \quad \text{and} \quad m_{\pi^\pm}^{*2} \simeq \frac{m_{\pi^\pm}^2}{1 - (\Lambda_{\rm PV} \pm \delta\Lambda_{\rm PV})}, \quad (67)$$

where

$$\left.\begin{aligned} \Lambda_{\rm PV} &= \mathcal{A} + B + C, \\ \delta\Lambda_{\rm PV} &= \frac{\mathcal{E}}{m_{\pi^\pm}}, \\ \gamma_{\pi\pi} &= 1 - \frac{\Lambda_{\rm PV}}{1-\Lambda_{\rm PV}} + \frac{\mathcal{B}}{1-\Lambda_{\rm PV}} + \frac{\mathcal{C}}{1-\Lambda_{\rm PV}}, \\ \alpha_{\pi\pi} &= \frac{\mathcal{A}}{1-\Lambda_{\rm PV}}, \\ \delta_{\pi\pi} &= \frac{\mathcal{D}}{1-\Lambda_{\rm PV}}. \end{aligned}\right\} \quad (68)$$

Note that if one uses Eq. (48) instead of Eq. (46), then $m_{\pi^{0,\pm}}^2$ and $\mathcal{C}$ will be replaced by $(m_{\pi^{0,\pm}}^2 + \mathcal{C}')$ and $\mathcal{D}'$, respectively, and $\delta_{\pi\pi}$ will vanish. Numerically, as mentioned before, Eqs. (46) and (48) give results very close to each other. Clearly from Eq. (61), $\mathcal{E}$ indicates that the asymmetry-driven mass splitting is of $\mathcal{O}(k_{p(n)}^5/M^{*4})$ for PV coupling.

Typical values of the pion mass shifts for PV coupling at normal nuclear density ($\rho_0 = 0.17$ fm^{-3}) for Pb-like nuclei are $\Delta m_{\pi^0} = 6.07$, $\Delta m_{\pi^+} = 4.6$, and $\Delta m_{\pi^-} = 8.02$ MeV with vacuum correction, and the corresponding values are 4.95, 3.47, and 6.82 MeV without vacuum correction.

In Fig. 7, we show results for the density dependence of effective pion masses for various charge states at $\alpha = 0.2$. It is observed that the π^- mass increases in matter, while π^+ decreases at higher density. The mass splitting is quite significant even at density $\rho \gtrsim 1.5\rho_0$. In the lower panel, we present results with vacuum corrections. Evidently the effect of vacuum corrections is small.

It should, however, be mentioned that the vacuum correction part for PV coupling is rather small. For loops involving heavy baryons it could be quite high. For detailed discussion, we refer the reader to Refs. [41,42]. In the present case, we take only the nucleon loop in the presence of the scalar mean field.

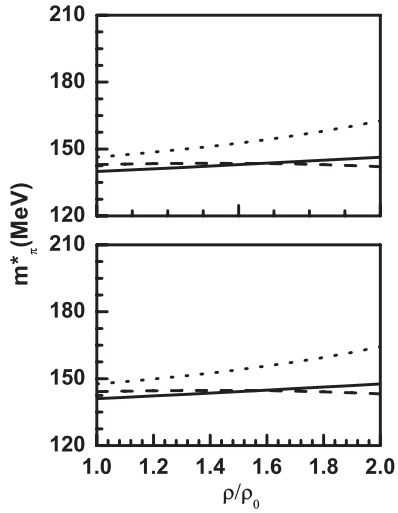

FIG. 7. Effective masses (for PV coupling) of π^0 (solid curve), π^+ (dashed curve), and π^- (dotted curve) are represented without the Dirac sea (upper panel) and with the Dirac sea (lower panel) at $\alpha = 0.2$.

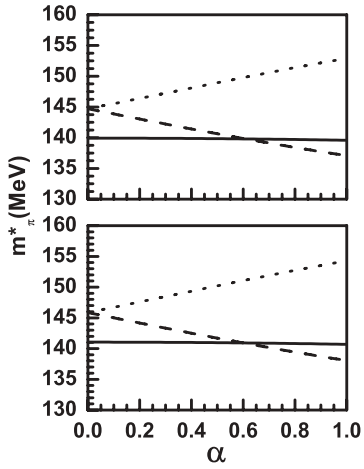

FIG. 8. Asymmetry parameter (α) dependent effective masses (for PV coupling) of π^0 (solid curve), π^+ (dashed curve), and π^- (dotted curve) at $\rho = 0.17\ \mathrm{fm}^{-3}$ without (upper panel) and with (lower panel) vacuum correction.

We also present results of asymmetry parameter dependence effective masses for different charge states of pion in Fig. 8 at normal nuclear matter density. The upper and lower panels present the effective pion masses without and with vacuum correction. It can be observed that the asymmetry parameter dependent pion mass splitting is insensitive to the vacuum correction. The pion dispersions in the medium for various charge states of pion are presented in Fig. 9 for PV coupling.

III. MODERN TECHNIQUE

In the previous sections, we have discussed pion propagation in ANM using both the PS and PV interaction within the framework of a nonchiral model. However, the interactions as represented by Eqs. (1) and (41) fail to describe in-medium

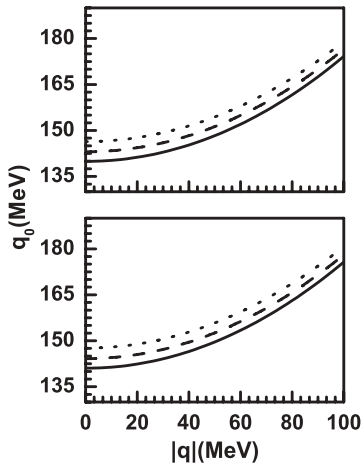

FIG. 9. Pion dispersion relation without (upper panel) and with (lower panel) the effect of the Dirac sea for PV coupling. The solid, dashed, and dotted curves, respectively, indicate the dispersion curves of π^0, π^+, and π^- at $\rho = 0.17\ \mathrm{fm}^{-3}$ and $\alpha = 0.2$.

πN dynamics as shown in Ref. [25]. It was also observed that the chirally symmetric model (linear) has also various limitations [25]. For example, as mentioned before, it fails to account for the pion-nucleus dynamics in nuclear matter in both the PS and PV representations. In fact, it gives too strong of a pion nucleon interaction in matter, which cannot be adjusted by fixing the s-wave π-N interaction in free space, even in the PV case. In this context, the Dirac vacuum involving baryon loops was found to play a significant role. If one uses the chiral model and breaks the symmetry explicitly, the results are found to be very sensitive to the renormalization scheme [25]. In Ref. [43], it was shown that the relativistic chiral model with a light scalar meson appears to provide an economical marriage of successful relativistic MFT and chiral symmetry. It, however, fails to reproduce the observed properties of finite nuclei, such as spin-orbit splittings, shell structure, charge densities, and surface energies. Since then, there has been a series of attempts to construct a model that has the virtue of describing both the properties of nuclear matter and finite nuclei [30,31,41,44–46]. Currently, the nonlinear chiral effective field theoretic approach seems to be quite successful in this respect. It might be recalled here that in such a framework, the explicit calculation of the Dirac vacuum is not required; on the contrary, here the short distance dynamics are absorbed into the parameters of the theory adjusted phenomenologically by fitting empirical data [30,31,42]. Now we proceed to calculate the effective pion masses in ANM in this approach.

By retaining only the lowest order terms in the pion fields, one obtains the following Lagrangian from the chirally invariant Lagrangian [31]:

$$\begin{aligned}\mathcal{L} = {} & \bar{\Psi}(i\gamma_\mu\partial^\mu - M)\Psi + g_s\bar{\Psi}\phi_s\Psi - g_\omega\bar{\Psi}\gamma_\mu\Phi^\mu_\omega\Psi \\ & - \frac{g_A}{f_\pi}\bar{\Psi}\gamma_5\gamma_\mu\partial^\mu\vec{\tau}\cdot\vec{\Phi}_\pi\Psi + \frac{1}{2}\left(\partial_\mu\Phi_s\partial^\mu\Phi_s - m_s^2\Phi_s^2\right) \\ & + \frac{1}{2}\left(\partial_\mu\vec{\Phi}_\pi\cdot\partial^\mu\vec{\Phi}_\pi - m_\pi^2\vec{\Phi}^2\right) - \frac{1}{4}G_{\mu\nu}G^{\mu\nu} \\ & + \frac{1}{2}m_\omega^2\Phi_{\omega\mu}\Phi^\mu_\omega + \mathcal{L}_{\mathrm{NL}} + \delta\mathcal{L}. \end{aligned} \tag{69}$$

The terms $\mathcal{L}_{\mathrm{NL}}$ and $\delta\mathcal{L}$ contain, respectively, the nonlinear terms of the meson sector and all of the counterterms. The explicit expressions for $\mathcal{L}_{\mathrm{NL}}$ and $\delta\mathcal{L}$ can be found in Ref. [31].

Note that the meson self-energy can be found by differentiating the energy density [31] at the two-loop level with respect to the meson propagator, as indicated in Fig. 10. One may, therefore, identify the FF, FD, and DD parts of the self-energy with the vacuum-fluctuation (VF), Lamb-shift (LS), and exchange (EX) contributions to the self-energy, respectively. The VF and LS terms are related to the short-range physics, while the EX part is related to the long-range physics. The detailed

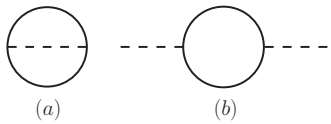

FIG. 10. Diagrams correspond to the two-loop self-energy and energy.

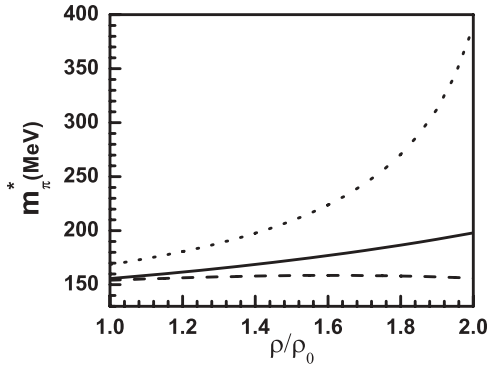

FIG. 11. Effective pion mass at different densities with $\alpha = 0.2$.

discussion about this short- and long-distance separation can be found in Refs. [30,31,42]. The diverging FF part of the self-energy and LS can be expressed as a sum of terms which already exists in the effective field theoretical Lagrangian and can be absorbed into the counterterms. The short-distance physics, as shown in Ref. [31], while calculating exchange energies, are either removed by field redefinitions or the coefficients are determined by fitting with the empirical data. The long-range part is computed explicitly, which produces modest corrections to the nuclear binding energy curve. This can be compensated for by a small adjustment of the coupling parameters.

Recently in Ref. [31], the exchange energy contributions of the pion have been calculated within this theoretical framework. We adopt the same parameter set as designated by "MOA" in Ref. [31] to calculate the π self-energy explicitly. The corresponding results are presented in Fig. 11. Here we simply depict the final results, because the expressions, at this order, for the pion self-energy and density-dependent masses of π^0 and $\pi^\pm$ remain the same as those of Eq. (67) except for the coupling parameters. Quantitatively, it is found that for the lower density, i.e., $\rho \sim \rho_0$, the effective masses for π^-, π^0, and π^+ states are comparable with those of PV coupling (Fig. 7); while at higher density, the mass splitting is significantly enhanced. The charged states, i.e., $\pi^\pm$, show stronger density dependence than in the PV coupling. We also observe that the density dependence of π^0 is rather weak.

IV. SUMMARY AND CONCLUSION

In the present paper, pion propagation in ANM has been studied within the framework of relativistic hadrodynamics in presence of the scalar mean field. We start with the model developed in Ref. [25], and present analytical results for the pion dispersion relations in ANM by making the HNL approximation and a suitable density expansion. Subsequently, we invoke the chirally invariant Lagrangian [47,48] by retaining only the lowest order terms in the pion field and compare the results with the nonchiral model calculations performed in Sec. II.

The splitting of the various charged states of pion even at normal nuclear matter density is found to be quite significant. Such mode splitting in ANM is, in fact, a generic feature of all the isovector mesons. Therefore, it would be interesting to estimate similar splitting for the ρ meson and other isovector states. It is to be noted that the mass splitting is related to the pion-nucleus optical potential [19,22]. As for the dispersion relations, we restricted our calculation to only the timelike region, which can also be extended to study the spacelike modes both for the pions and ρ mesons.

ACKNOWLEDGMENTS

The authors gratefully thank Pradip Roy and Kausik Pal for valuable comments and suggestions.

APPENDIX A

After using the Feynman parametrization, the term $\Sigma^{*\mathrm{FF}}_{\mathrm{PS}}(q)$ in Eq. (15) can be written as

$$\begin{aligned}
\Sigma^{*\mathrm{FF}}_{\mathrm{PS}}(q) &= 8ig_\pi^2\mu^{2\epsilon}\int\frac{d^Nk}{(2\pi)^N}\int_0^1 dx \\
&\quad\times\left[\frac{M^{*2}-k\cdot(k+q)}{((k+qx)^2+q^2x(1-x)-M^{*2})^2}\right] \\
&= \frac{g_\pi^2}{2\pi^2}\int_0^1 dx(4\pi\mu^2)^\epsilon\frac{\Gamma(\epsilon)}{1-\epsilon} \\
&\quad\times\left[\frac{M^{*2}-3q^2x(1-x)+2\epsilon q^2x(1-x)}{(M^{*2}-q^2x(1-x))^\epsilon}\right] \\
&= \frac{g_\pi^2}{2\pi^2}\frac{q^2}{3}+\frac{g_\pi^2}{2\pi^2}\frac{1}{\epsilon}\left(M^{*2}-\frac{q^2}{2}\right) \\
&\quad-\frac{g_\pi^2}{2\pi^2}\left(M^{*2}-\frac{q^2}{2}\right)(\gamma_E'-\ln(4\pi\mu^2)) \\
&\quad-\frac{g_\pi^2}{2\pi^2}\int_0^1 dx(M^{*2}-3q^2x(1-x)) \\
&\quad\times\ln(M^{*2}-q^2x(1-x)).
\end{aligned} \tag{A1}$$

Here $\epsilon = 2-\frac{N}{2}$ and μ is an arbitrary scaling parameter. γ_E is the Euler-Mascheroni constant and $\gamma_E' = (\gamma_E - 1)$. The imaginary part of $\Sigma^{*\mathrm{FF}}_{\mathrm{PS}}(q)$ can easily be found by simply replacing $\ln(M^{*2}-q^2x(1-x))$ with $\ln(M^{*2}-q^2x(1-x)-i\eta)$, where η is an arbitrarily small parameter and the term $i\eta$ comes from the denominator of G_i^F when the Feynman parametrization is performed considering $i\zeta$ in the denominator of the propagator.

Here the term $\ln(M^{*2}-q^2x(1-x))$ has a branch cut only for $M^{*2}-q^2x(1-x)<0$, and it begins at $q^2 = 4M^{*2}$, i.e., the threshold condition for nucleon-antinucleon pair production. So the limit of the x integration changes from (0,1) to $(\frac{1}{2}-\frac{1}{2}\alpha, \frac{1}{2}+\frac{1}{2}\alpha)$, where $\alpha = \sqrt{1-\frac{4M^{*2}}{q^2}}$, and we used $\mathrm{Im}\ln(Z-i\eta) = -\pi$. Now,

$$\int_{\frac{1}{2}-\frac{1}{2}\alpha}^{\frac{1}{2}+\frac{1}{2}\alpha} dx\,\theta(q^2-4M^{*2}) = \sqrt{1-\frac{4M^{*2}}{q^2}}\theta(q^2-4M^{*2}). \tag{A2}$$

Now, the imaginary part of $\Sigma^{*\mathrm{FF}}_{\mathrm{PS}}(q)$ is

$$\begin{aligned}\mathrm{Im}\Sigma^{*\mathrm{FF}}_{\mathrm{PS}}(q) &= -\frac{g_\pi^2}{2\pi^2}\int_0^1 dx(M^{*2}-3q^2x(1-x)) \\ &\quad\times \mathrm{Im}[\ln(M^{*2}-q^2x(1-x)-i\eta)] \\ &= -\frac{g_\pi^2}{4\pi}[q\sqrt{q^2-4M^{*2}}]\theta(q^2-4M^{*2}). \qquad \text{(A3)}\end{aligned}$$

It is clear from the expression of Eq. (A1) that the second term is divergent in the limit $\epsilon \to 0$ (as $N \to 4$). To remove the divergences, we need to add the counterterms [25] in the original Lagrangian interaction. The diverging part of Eq. (A1) is

$$\begin{aligned}\mathcal{D}_{\mathrm{PS}} &= \frac{g_\pi^2}{2\pi^2}\frac{1}{\epsilon}\left(M^{*2}-\frac{q^2}{2}\right) \\ &= \frac{g_\pi^2}{2\pi^2}\left[\frac{M^2}{\epsilon}-\frac{2}{\epsilon}Mg_s\phi_0+\frac{1}{\epsilon}g_s^2\phi_0^2-\frac{q^2}{2\epsilon}\right]. \qquad \text{(A4)}\end{aligned}$$

In Eq. (A4) we substitute the effective nucleon mass $M^* = (M - g_s\phi_0)$, where M is the nucleon mass and ϕ_0 is the vacuum expectation value of the scalar field ϕ_s. The expression given in Eq. (A4) tells us that we need to add four counterterms [25] with the original interaction Lagrangian to remove the divergences from $\Sigma^{*\mathrm{FF}}_{\mathrm{PS}}$. Therefore, the counterterm Lagrangian [25] is denoted as

$$\begin{aligned}\mathcal{L}_{\mathrm{CT}} &= -\frac{1}{2!}\beta_1\Phi_\pi\cdot\left(\partial^2+m_\pi^2\right)\cdot\Phi_\pi+\frac{1}{2!}\beta_2\Phi^2+\frac{1}{2!}\beta_3\phi_s\Phi_\pi^2 \\ &\quad+\frac{1}{2!2!}\beta_4\phi^2\Phi_\pi^2. \qquad \text{(A5)}\end{aligned}$$

The value of the counterterms β_1, β_2, β_3, and β_4 are determined by imposing the appropriate renormalization conditions, that is,

$$\beta_1 = \left(\frac{\partial\Sigma^{\mathrm{FF}}_{\mathrm{PS}}(q)}{\partial q^2}\right)_{q^2=m_\pi^2}, \qquad \text{(A6)}$$

$$\beta_2 = \left(\Sigma^{\mathrm{FF}}_{\mathrm{PS}}\right)_{q^2=m_\pi^2}, \qquad \text{(A7)}$$

$$\beta_3 = -g_s\left(\frac{\partial\Sigma^{\mathrm{FF}}_{\mathrm{PS}}(q)}{\partial M}\right)_{q^2=m_\pi^2}, \qquad \text{(A8)}$$

$$\beta_4 = -\delta\lambda + g_s^2\left(\frac{\partial^2\Sigma^{\mathrm{FF}}_{\mathrm{PS}}(q)}{\partial M^2}\right)_{q^2=m_\pi^2}. \qquad \text{(A9)}$$

Here β_1 and β_2 are the wave function and pion mass renormalization counterterms, respectively, while β_3 and β_4 are the vertex renormalization counterterms for the $\phi_s\Phi_\pi^2$ vertex and $\phi_s^2\Phi_\pi^2$ vertex, respectively. The conditions of Eqs. (A6) and (A7) imply that the pion propagator $G_\pi = [q^2 - m_\pi^2 - \Sigma^{*R}_{\mathrm{PS}}(q)]^{-1}$ reproduces the physical mass of pions in free space. The counterterm β_4 determines the strength of coupling of the $\phi_s^2\Phi_\pi^2$ vertex. In fact, $\Sigma^{\mathrm{FF}}_{\mathrm{PS}}(q)$ is found by simply replacing M^* with M in Eq. (A1). We can set $\delta\lambda = 0$ to minimize the effects of many-body forces in the nuclear medium [25], which is consistent with the renormalization scheme for scalar meson. Using the conditions given in Eqs. (A6)–(A9), the following results are found:

$$\begin{aligned}\beta_1 &= \frac{g_\pi^2}{2\pi^2}\left[\frac{1}{3}-\frac{1}{2}\left(\frac{1}{\epsilon}-\gamma_E'+\ln(4\pi\mu^2)\right)\right] \\ &\quad+\frac{g_\pi^2}{2\pi^2}\left[\int_0^1 dx3x(1-x)\ln\left(M^2-m_\pi^2x(1-x)\right)\right] \\ &\quad+\frac{g_\pi^2}{2\pi^2}\left[\int_0^1 dx\ \frac{M^2x(1-x)-3m_\pi^2x^2(1-x)^2}{M^2-m_\pi^2x(1-x)}\right], \qquad \text{(A10)}\end{aligned}$$

$$\begin{aligned}\beta_2 &= \frac{g_\pi^2}{2\pi^2}\left[\frac{m_\pi^2}{2}+\left(M^2-\frac{m_\pi^2}{3}\right)\left(\frac{1}{\epsilon}-\gamma_E'+\ln(4\pi\mu^2)\right)\right] \\ &\quad-\frac{g_\pi^2}{2\pi^2}\left[\int_0^1 dx\left(M^2-3m_\pi^2x(1-x)\right)\right. \\ &\quad\left.\times\ln\left(M^2-m_\pi^2x(1-x)\right)\right], \qquad \text{(A11)}\end{aligned}$$

$$\begin{aligned}\beta_3 &= \frac{g_\pi^2}{2\pi^2}\left[-g_s(2M)\left(\frac{1}{\epsilon}-\gamma_E'+\ln(4\pi\mu^2)\right)\right] \\ &\quad+\frac{g_\pi^2}{2\pi^2}\left[g_s(2M)\int_0^1 dx\ln\left(M^2-m_\pi^2x(1-x)\right)\right] \\ &\quad+\frac{g_\pi^2}{2\pi^2}\left[g_s(2M)\int_0^1 dx\left(\frac{M^2-3m_\pi^2x(1-x)}{M^2-m_\pi^2x(1-x)}\right)\right], \qquad \text{(A12)}\end{aligned}$$

$$\begin{aligned}\beta_4 &= -\frac{g_\pi^2}{2\pi^2}6g_s^2+\frac{g_\pi^2}{2\pi^2}\left[2g_s\left(\frac{1}{\epsilon}-\gamma_E'+\ln(4\pi\mu^2)\right)\right] \\ &\quad-\frac{g_\pi^2}{2\pi^2}\left[2g_s^2\int_0^1 dx\ln\left(M^2-m_\pi^2x(1-x)\right)\right] \\ &\quad-\frac{g_\pi^2}{2\pi^2}\left[2g_s^2\int_0^1 dx\ \frac{4M^2m_\pi^2x(1-x)}{\left(M^2-m_\pi^2x(1-x)\right)^2}\right]. \qquad \text{(A13)}\end{aligned}$$

Now the renormalized $\Sigma^{*\mathrm{FF}}_{\mathrm{PS}}(q)$ is

$$\begin{aligned}\Sigma^{*R}_{\mathrm{PS}}(q,m_\pi) &= \Sigma^{*\mathrm{FF}}_{\mathrm{PS}}(q)-\beta_1\left(q^2-m_\pi^2\right) \\ &\quad-\beta_2-\beta_3\phi_0-\tfrac{1}{2}\beta_4\phi_0^2. \qquad \text{(A14)}\end{aligned}$$

Substituting $\Sigma^{*\mathrm{FF}}_{\mathrm{PS}}(q)$ from Eq. (A1) and $\beta_1, \beta_2, \beta_3, \beta_4$ from Eqs. (A10)–(A13) into Eq. (A14), it is found that the divergences in $\Sigma^{*\mathrm{FF}}_{\mathrm{PS}}(q)$ are completely eliminated by the counterterms. After simplification, $\Sigma^{*R}_{\mathrm{PS}}(q,m_\pi)$ reduces to

$$\begin{aligned}&\Sigma^{*R}_{\mathrm{PS}}(q,m_\pi) \\ &= \frac{g_\pi^2}{2\pi^2}\left[-3(M^2-M^{*2})+\left(q^2-m_\pi^2\right)\left(\frac{1}{6}+\frac{M^2}{m_\pi^2}\right)\right. \\ &\quad-2M^{*2}\ln\left(\frac{M^*}{M}\right)+\frac{8M^2(M-M^*)^2}{\left(4M^2-m_\pi^2\right)} \\ &\quad\left.-\frac{2M^{*2}\sqrt{4M^{*2}-q^2}}{q}\tan^{-1}\left(\frac{q}{\sqrt{4M^{*2}-q^2}}\right)\right.\end{aligned}$$

$$+\frac{2M^2\sqrt{4M^2-m_\pi^2}}{m_\pi}\tan^{-1}\left(\frac{m_\pi}{\sqrt{4M^2-m_\pi^2}}\right)$$
$$+\left((M^2-M^{*2})+\frac{m_\pi^2(M-M^*)^2}{(4M^2-m_\pi^2)}+\frac{M^2}{m_\pi^2}(q^2-m_\pi^2)\right)$$
$$\times\frac{8M^2}{m_\pi\sqrt{4M^2-m_\pi^2}}\tan^{-1}\left(\frac{m_\pi}{\sqrt{4M^2-m_\pi^2}}\right)$$
$$+\int_0^1 dx\,3x(1-x)q^2\ln\left(\frac{M^{*2}-q^2x(1-x)}{M^2-m_\pi^2x(1-x)}\right)\Bigg]. \quad \text{(A15)}$$

APPENDIX B

After Feynman parametrization, Eq. (44) reduces to

$$\Sigma_{\rm PV}^{*\rm FF}(q)$$
$$=8i\left(\frac{f_\pi}{m_\pi}\right)^2\mu^{2\epsilon}\int\frac{d^Nk}{(2\pi)^N}\int_0^1 dx$$
$$\times\left[\frac{(M^{*2}+q^2x(1-x)+k^2)q^2-2(k\cdot q)^2}{((k+qx)^2+q^2x(1-x)-M^{*2})^2}\right]$$
$$=-\frac{q^2}{2\pi^2}\left(\frac{f_\pi}{m_\pi}\right)^2\int_0^1 dx(4\pi\mu^2)^\epsilon\Gamma(\epsilon)$$
$$\times\left[\frac{2M^{*2}}{(M^{*2}-q^2x(1-x))^\epsilon}\right]$$
$$=\frac{q^2}{2\pi^2}\left(\frac{f_\pi}{m_\pi}\right)^2[2M^{*2}(\gamma_E-\ln(4\pi\mu^2))]$$
$$+\frac{q^2}{2\pi^2}\left(\frac{f_\pi}{m_\pi}\right)^2\left[2M^{*2}\int_0^1 dx\ln(M^{*2}-q^2x(1-x))\right]$$
$$-\frac{q^2}{2\pi^2}\left(\frac{f_\pi}{m_\pi}\right)^2\left[\frac{2M^{*2}}{\epsilon}\right] \quad \text{(B1)}$$

The imaginary part of $\Sigma_{\rm PV}^{*\rm FF}(q)$ can be found as

$$\mathrm{Im}\,\Sigma_{\rm PV}^{*\rm FF}(q)$$
$$=-\left(\frac{f_\pi}{m_\pi}\right)^2\left[\frac{q}{\pi}2M^{*2}\sqrt{q^2-4M^{*2}}\right]\theta(q^2-4M^{*2}). \quad \text{(B2)}$$

It is clear from Eq. (B2) that $\mathrm{Im}\Sigma_{\rm PV}^{*\rm FF}(q)$ vanishes for $q^2 < 4M^{*2}$. With the same argument as stated for PS coupling, we excluded the imaginary part. The diverging part of $\Sigma_{\rm PV}^{*\rm FF}(q)$ is

$$\mathcal{D}_{\rm PV}=-\frac{q^2}{2\pi^2}\left(\frac{f_\pi}{m_\pi}\right)^2\left[\frac{2M^{*2}}{\epsilon}\right]. \quad \text{(B3)}$$

Here we use simple subtraction to remove the divergence. So, the finite FF part of the self-energy is

$$\Sigma_{\rm PV}^{*R}(q)=\Sigma_{\rm PV}^{*\rm FF}(q)-\Sigma_{\rm PV}^{*\rm FF}(m_\pi)=\frac{q^2}{2\pi^2}\left(\frac{f_\pi}{m_\pi}\right)^2$$
$$\times\left[2M^{*2}\int_0^1 dx\ln\left(\frac{M^{*2}-q^2x(1-x)}{M^{*2}-m_\pi^2x(1-x)}\right)\right]. \quad \text{(B4)}$$

[1] A. B. Migdal, Rev. Mod. Phys. **50**, 107 (1978).
[2] I. M. Mishustin, F. Myhrer, and P. J. Siemens, Phys. Lett. **B95**, 361 (1980).
[3] M. Gyulassy and W. Greiner, Ann. Phys. (N.Y.) **109**, 485 (1977).
[4] G. E. Brown, E. Oset, M. Vicente Vacas, and W. Weise, Nucl. Phys. **A505**, 823 (1989).
[5] L. H. Xia, C. M. Ko, L. Xiong, and J. Q. Wu, Nucl. Phys. **A485**, 721 (1988).
[6] C. Gale and J. I. Kapusta, Phys. Rev. C **35**, 2107 (1987).
[7] E. Oset, H. Toki, and W. Weise, Phys. Rept. **83**, 281 (1982).
[8] A. B. Migdal, E. E. Saperstein, M. A. Troitsky, and D. N. Voskresensky, Phys. Rep. **192**, 179 (1990).
[9] V. F. Dmitriev and T. Suzuki, Nucl. Phys. **A438**, 697 (1985).
[10] P. A. Henning and H. Umezawa, Nucl. Phys. **A571**, 617 (1994).
[11] C. L. Korpa and R. Malfliet, Phys. Rev. C **52**, 2756 (1995).
[12] J. Helgesson and J. Randrup, Phys. Rev. C **52**, 427 (1995).
[13] L. Liu and M. Nakano, Nucl. Phys. **A618**, 337 (1997).
[14] T. Herbert, K. Wehrberger, and F. Beck, Nucl. Phys. **A541**, 699 (1992).
[15] J. D. Walecka, Ann. Phys. (N.Y.) **83**, 491 (1974).
[16] R. Rapp and J. Wambach, Adv. Nucl. Phys. **25**, 1 (2000).
[17] C. Y. Wong, *Introduction to High-Energy Heavy-Ion Collisions* (World Scientific, Singapore, 1994).
[18] G. Chanfray and P. Schuck, Nucl. Phys. **A555**, 329 (1993).
[19] N. Kaiser and W. Weise, Phys. Lett. **B512**, 283 (2001).
[20] P. Costa, M. C. Ruivo, and Yu. L. Kalinovsky, Phys. Lett. **B560**, 171 (2003).
[21] P. Costa, M. C. Ruivo, C. A. de Sousa, and Yu. L. Kalinovsky, Phys. Rev. C **70**, 025204 (2004).
[22] S. Biswas and A. K. Dutt-Mazumder, Phys. Rev. C **74**, 065205 (2006).
[23] B. D. Serot, Phys. Lett. **B86**, 146 (1979); **B87**, 403(E) (1979).
[24] J. I. Kapusta, Phys. Rev. C **23**, 1648 (1981).
[25] T. Matsui and B. D. Serot, Ann. Phys. (N.Y.) **144**, 107 (1982).
[26] S. Weinberg, Phys. Rev. Lett. **18**, 188 (1967).
[27] S. Weinberg, Phys. Rev. **166**, 1568 (1968).
[28] S. Weinberg, Physica (Utrecht) A **96**, 327 (1979).
[29] J. Schwinger, Phys. Lett. **B24**, 473 (1967).
[30] B. D. Serot and J. D. Walecka, Int. J. Mod. Phys. E **6**, 515 (1997).
[31] Y. Hu, J. McIntire, and B. D. Serot, Nucl. Phys. **A794**, 187 (2007).
[32] C. J. Horowitz and B. D. Serot, Nucl. Phys. **A368**, 503 (1981).
[33] M. Schäfer, H. C. Dönges, A. Engel, and U. Mosel, Nucl. Phys. **A575**, 429 (1994).
[34] B. D. Serot and J. D. Walecka, Adv. Nucl. Phys. **16**, 1 (1986).
[35] S. A. Chin, Ann. Phys. (N.Y.) **108**, 301 (1977).
[36] G. 't Hooft and M. T. Veltman, Nucl. Phys. **B44**, 189 (1973).
[37] M. E. Peskin and D. V. Schroeder, *An Introduction to Quantum Field Theory* (Addison-Wesley, Reading, MA, 1995).

[38] T. P. Cheng and L. F. Li, *Gauge Theory of Elementary Particles* (Clarendon, Oxford, 2006).
[39] A. K. Dutt-Mazumder, Nucl. Phys. **A713**, 119 (2003).
[40] T. Ericson and W. Weise, *Pions and Nuclei* (Oxford University, New York, 1988).
[41] R. J. Furnstahl, H. B. Tang, and B. D. Serot, Phys. Rev. C **52**, 1368 (1995).
[42] R. J. Furnstahl, R. J. Perry, and B. D. Serot, Phys. Rev. C **40**, 321 (1989).
[43] R. J. Furnstahl and B. D. Serot, Phys. Rev. C **47**, 2338 (1993).
[44] R. J. Furnstahl, C. E. Price, and G. E. Walker, Phys. Rev. C **36**, 2590 (1987).
[45] R. J. Furnstahl and B. D. Serot, Phys. Lett. **B316**, 12 (1993).
[46] R. J. Furnstahl, B. D. Serot, and H. B. Tang, Nucl. Phys. **A598**, 539 (1996).
[47] R. J. Furnstahl, B. D. Serot, and H. B. Tang, Nucl. Phys. **A615**, 441 (1997).
[48] R. J. Furnstahl, B. D. Serot, and H. B. Tang, Nucl. Phys. **A640**, 505(E) (1998).